

#### **MALAYSIAN JOURNAL OF ANALYTICAL SCIENCES**



Journal homepage: https://mjas.analis.com.my/

### Research Article

# Cold flow improvement of large-branched esterified palm olein for potential green lubricant

Loh Lii Jia<sup>1\*</sup>, Diana Kertini Monir<sup>1\*</sup>, and Mohamad Iskandar Jobli<sup>2</sup>

Received: 6 November 2024; Revised: 23 March 2025; Accepted: 23 March 2025; Published: 19 June 2025

#### Abstract

The poor cold flow properties of natural palm olein (PO<sub>o</sub>) limit its application at low temperature environments, particularly in automotive and industrial fluids. This constraint highlights the need for further research to develop value-added lubricants. To address this issue, the olefinic structure of PO<sub>o</sub> was transformed to large-branched esters through epoxidation, alcoholysis, and esterification. A key step involved the use of glycerol for epoxide ring opening enabling the incorporation of three hydroxyl groups to facilitate the formation of large-branched esters. Epoxidation of PO<sub>o</sub> with performic acid resulted in epoxidized PO<sub>o</sub> (EPO<sub>o</sub>) with a 90.65% yield and 98.14% oxirane conversion. The subsequent ring-opening reaction with glycerol produced a ring-opening intermediate with 85.93% yield. Esterification was performed using oleic acid, linoleic acid, and salicylic acid under optimal condition of 140°C for 4 hours yielding oleic acid-esterified-PO<sub>o</sub> (OA-EPO), linoleic acid-esterified-PO<sub>o</sub> (LA-EPO), and salicylic acid-esterified-PO<sub>o</sub> (SA-EPO) at 97.46%, 96.19%, and 99.29%, respectively. The products were characterised using the Fourier Transform Infrared (FTIR) spectroscopy, proton (¹H), and carbon (¹³C) Nuclear Magnetic Resonance (NMR) spectroscopy. The results demonstrated a significant improvement in cold flow properties, with a temperature range of -12°C to -7°C, compared to natural PO<sub>o</sub> at 6°C. These findings provide valuable insights into the potential of large-branched esterified PO<sub>o</sub> as a versatile green lubricant that can operate at low-temperature environments.

Keywords: Palm olein, epoxidation, alcoholysis, esterification, green lubricant

#### Introduction

Since the Industrial Revolution, the global economy has largely relied on factory manufacturing, including the production of essential products, such as lubricating oils. In the industrial era, lubricants for energy became indispensable optimising consumption, reducing friction, minimising mechanical wear, and preventing corrosion, all of which are crucial for ensuring extended machine performance. The global bio-lubricant market is experiencing significant growth, projected to rise from 1.9 billion USD in 2020 to 2.5 billion USD by 2026 within the U.S. lubricant market, with a Compound Annual Growth Rate (CAGR) of 5.2% [1]. In terms of regional distribution, most lubricants are supplied to the Asia-Pacific region (35%), followed by Europe (23%), North America (22%), Latin America (10%), Africa (6%), and the Middle East (4%) [2]. Despite the increasing demand for bio-lubricants, modern machinery predominantly relies on mineral-based lubricants due to their high operating efficacy. Nevertheless, these mineral-based lubricants pose significant environmental challenges that are hazardous, non-renewable, and exhibit low biodegradability, contributing to the discharge of over 24 million tonnes of waste oil globally every year [2, 3].

Considering sustainability concerns, the extraction of crude oil from the Earth's crust to meet the industrial demands for lubricants raises alarm, as this natural resource may eventually become depleted. Therefore, raising public awareness about alternative lubricants is critical to preserving refined crude oil for technological purposes. Recent studies have presented vegetable oil-based lubricants as a promising

<sup>&</sup>lt;sup>1</sup>Department of Chemistry, Faculty of Resource Science and Technology, University Malaysia Sarawak, 94300 Kota Samarahan, Sarawak, Malaysia

<sup>&</sup>lt;sup>2</sup>Department of Mechanical and Manufacturing Engineering, Faculty of Engineering, University Malaysia Sarawak, 94300 Kota Samarahan, Sarawak, Malaysia

<sup>\*</sup>Corresponding author: liijia.loh@gmail.com

alternative to petroleum-based lubricants due to their high biodegradability and low toxicity [4]. Nevertheless, the widespread application of plant oilbased lubricant remains limited, hence, further study is required to explore the potential of vegetable oils, such as palm olein, in producing sustainable green lubricants.

Palm olein (PO<sub>0</sub>) has significant potential as an alternative green lubricant through chemical modification techniques due to its high content of long-chain fatty acids, such as oleic acid (44%) and linoleic acid (13%). These long-chain fatty acids are ideal to be further processed into lubricants [5]. The amphiphilic molecules in the POo belong to the polar ester groups associated at the non-polar hydrocarbon chains. These amphiphilic molecules in PO<sub>o</sub> comprise of polar ester groups that are attached to non-polar hydrocarbon chains, which exhibit properties that meet the requirements for both boundary and hydrodynamic lubrication [5, 6]. As a renewable and less hazardous resource, POo has the potential to replace up to 90% of petroleum-based oils, thereby, reducing the non-recyclable waste [6, 7]. Malaysia is known as the world's second-largest producer of palm, with 5.9 million hectares of oil palm plantations and 423 operational palm oil factories [8]. These factors position POo as a viable and sustainable feedstock for bio-lubricant, supporting the growing demand for lubricants in various applications, such as reducing abrasion, ensuring effective lubrication, and forming protective films between machine surfaces.

Despite the outstanding advantages of PO<sub>o</sub>, this vegetable-based oil faces a critical limitation in its poor cold flow properties. This drawback restricts its application as a lubricant in the refrigeration system within the food industry and in colder climates, where it tends to solidify at lower temperatures [9]. Saturated fatty acids present in vegetable-based oil are more prone to forming macro-crystals than their unsaturated counterparts [4]. The solidification occurs primarily in the linear triacylglycerols of the oil due to its uniform molecular structure that facilitates the formation of crystal lattices through nucleation or crystallisation under cold conditions.

To address the issue of poor cold flow properties, the chemical modification of  $PO_0$  was proposed through the incorporation of ester moiety via epoxidation, alcoholysis, and esterification reactions [10]. Epoxidation is widely recognised as an effective strategy for introducing epoxide groups due to its simplicity, cost-effectiveness and high selectivity. During the epoxidation process, the unsaturated triglycerides in  $PO_0$  react with the reactive peracid reagents, such as performic or peracetic acid.

Performic acid is produced *in situ* by adding hydrogen peroxide (H<sub>2</sub>O<sub>2</sub>) to formic acid (HCOOH), where the H<sub>2</sub>O<sub>2</sub> acts as an oxygen donor and HCOOH serves as an oxygen carrier [11,12]. The use of H<sub>2</sub>O<sub>2</sub> is highly efficient as an active oxygen source and is environmentally friendly, producing only water as the primary byproduct during the epoxidation [13]. Nevertheless, increasing the concentration of H<sub>2</sub>O<sub>2</sub> can lead to side reactions, including oxirane rings damage, emphasising the need to optimise the molar ratio of reagents [14]. Nor et al. [15] reported that the optimal conditions for epoxidation involved a 5.91 molar ratio of formic acid to 3.60 molar ratio of H<sub>2</sub>O<sub>2</sub>, conducted at 40°C for 2.55 hours, achieving an 86% yield. Other than concentration, temperature also plays a crucial role in the efficiency of epoxidation. According to Yunus et al. [16], a higher conversion percentage was observed at 45°C (5.55%) than 60°C (2.22%). The reduction of epoxy content at elevated temperatures could be due to oxirane cleavage that was likely caused by partial hydrolysis and subsequent degradation of the epoxy groups [16].

To enhance the oil's performance, the ring-opening reaction via alcoholysis is performed following the epoxidation. The alcoholysis process involves opening the oxirane ring of epoxidized fatty acids using various nucleophiles, such as alcohols, in the presence of catalysts to produce ring-opening intermediates. Glycerol was selected as the ringopening reagent in this study to introduce additional hydroxyl groups, facilitating the formation of largebranched esters and increasing the spacing between triglyceride molecules. Glycerol, with two primary and one secondary hydroxyl groups, is particularly effective in the ring opening process, as the primary hydroxyl groups have a higher reactivity in forming bio-polyols [17, 18]. While epoxidation and ring opening reactions improved some chemical properties of the oil, its poor cold flow behaviour persisted, necessitating an esterification step. This esterification reaction benefits from higher activation energy to accelerate the rate and achieve equilibrium, which allows better access to the catalyst's inner pores [19, 20].

In this study, it is postulated with more installation of ester moieties between triglycerides of palm olein, the larger branched structures will drastically disrupt the crystallization process at very low temperature. This improvement will widen its application in many areas as it is expected to demonstrate good cold flow relative to natural palm olein. Therefore, this project aimed to synthesize and characterize large branched-esterified palm olein by epoxidation, alcoholysis, and esterification with different carboxylic acids. The effect of large-branched esterified palm olein towards

their cold flow behaviour was investigated based on pour point values.

### Materials and Methods Materials

The vegetable oil of palm olein (PO<sub>o</sub>) (Buruh brand, Lam Soon Edible Oils Sdn. Bhd.) was procured from the local market and used as the raw material in this study. Chemicals such as formic acid (90% HCOOH), hydrogen peroxide (50% H<sub>2</sub>O<sub>2</sub>), glycerol (99.8%), hydrochloric acid (37% HCl), and paraffin liquid were sourced from R&M Chemicals. The boron trifluoride diethyl ether complex (50% BF<sub>3</sub>·Et<sub>2</sub>O), oleic acid (99%), and linoleic acid (99%) were obtained from Sigma-Aldrich. Salicylic acid (99.5%), ethyl acetate (99.95%), and sodium bicarbonate (99.5% NaHCO<sub>3</sub>) were supplied by Bendosen laboratory chemicals while the anhydrous magnesium sulphate (98% MgSO<sub>4</sub>) and potassium hydroxide pellets Grade AR (85%) were purchased from QREC Sdn. Bhd., Malaysia. Sulfuric acid (95% H<sub>2</sub>SO<sub>4</sub>), toluene (99.5%), and ethanol (99.5%) were obtained from EMSURE, Systerm, and HmbG, respectively. Sodium chloride (99.8% NaCl) and anhydrous calcium chloride (96% CaCl<sub>2</sub>) were purchased from Uni-Chem, while deuterated chloroform (99.75% CDCl<sub>3</sub>) and acetonitrile (99.9%) were purchased from Acros Organics and J.T. Baker, respectively.

# **Epoxidation**

The preparation of epoxides followed the method developed by Nor et al. [15]. Epoxidation was carried out by mixing PO<sub>o</sub> (50.0 g, 58.5 mmol, 0.0585 equivalent) with HCOOH (17.691 g, 384.4 mmol, 0.384 equivalent) in a 250 mL single-necked round bottom flask fitted with a reflux condenser. H<sub>2</sub>O<sub>2</sub> (14.334 g, 421.9 mmol, 0.844 equivalent) was added dropwise at a flow rate of 2 mL min<sup>-1</sup> under continuous magnetic stirring (900 rpm). The reaction was exothermic, so it was monitored regularly in the ice bath (4°C). The molar ratio of POo: HCOOH: H2O2 was fixed at optimum of 1: 5.91: 3.60 [15]. The epoxidation was optimised by varying the reaction temperature (30-60°C) and reaction time (30-153 minutes). The reaction progress was monitored based on the oxirane oxygen content (OOC) until it exceeded 90% of the theoretical value. After completion, the reaction mixture was cooled to room temperature and neutralised sequentially with 5% NaHCO<sub>3</sub> solution (100 mL) and 5% NaCl solution (100 mL), The product was extracted into 100mL of ethyl acetate, and the organic layer was separated using a separating funnel. The organic phase was dried over anhydrous MgSO<sub>4</sub>, filtered and concentrated in vacuo to yield the crude product EPO<sub>o</sub> (47.874 g, 90.65%) as yellowish-white oil.

#### Ring opening reaction via alcoholysis

The alcoholysis reaction was initiated by mixing EPO<sub>o</sub> (50.0 g, 55.4 mmol, 0.0554 equivalent) and glycerol (51.132 g, 555.6 mmol, 0.556 equivalent) in a 250 mL single-necked round-bottom flask fitted with a reflux condenser. The mixture was stirred and preheated to 120°C. The catalyst of BF<sub>3</sub>·Et<sub>2</sub>O (7.864 g, 55.4 mmol, 0.166 equivalent) was then added dropwise into the mixture. The molar ratio of EPOo, glycerol, and BF<sub>3</sub>·Et<sub>2</sub>O remained at 1: 10: 1 [23]. The reaction parameters were optimised by varying the reaction time (1-6 hours) and temperature (90-120°C). The OOC analysis was conducted every 60 minutes to monitor the progress until the OOC percentage dropped below 0.1%. Upon completion, the mixture was neutralised sequentially with 100 mL of 5% NaCl solution and 100 mL of 5% NaHCO<sub>3</sub> solution. The neutralised product was then diluted with 100 mL of ethyl acetate, and the pH was adjusted to pH 5-6. The organic layer was separated from the aqueous layer using a separating funnel, dried over anhydrous MgSO<sub>4</sub>, filtered and concentrated under reduced pressure. The polyols were yielded as the yelloworange oil (56.389 g, 85.93%).

#### Esterification

The esterification reaction was performed based on the protocol developed by Nor and Salimon [21] using three different starting materials, such as salicylic acid, oleic acid, and linoleic acid. Slight modifications were made where 0.237 mL of 95% H<sub>2</sub>SO<sub>4</sub> (0.436 g, 4.44 mmol, 0.009 equivalent) was used as a catalyst. Salicylic acid (0.586 g, 4.25 mmol, 0.004 equivalent) was dissolved in 100 mL of toluene at room temperature and the mixture was stirred continuously at 200 rpm for 1 h to ensure complete protonation. The solution was then transferred to a round-bottom flask containing polyols (5.0 g, 4.23 mmol, 0.004 equivalent). Then, the mixture was refluxed at temperatures ranging 80 to 140°C for 2-6 hours to optimise the reaction. The molar ratio of polyols, salicylic acid, and sulphuric acid was maintained at 1:4:1. The mixture was then cooled to room temperature and sequentially neutralised with 100 mL each of 5% NaCl solution and 5% NaHCO<sub>3</sub> solution. The mixture was then diluted with 100 mL of ethyl acetate until the pH was adjusted to pH 6-7. The organic layer was separated from the aqueous layer using a separating funnel, dried over anhydrous MgSO<sub>4</sub>, filtered, and concentrated under reduced pressure to yield the desired ester as a dark oil (9.497 g, 99.29%).

The same procedure was repeated with oleic acid (1.205 g, 4.26 mmol, 0.004 equivalent) and linoleic acid (1.196 g, 4.26 mmol, 0.004 equivalent) as starting materials to react with polyols (5.0 g, 4.23 mmol,

0.004 equivalent). These reactions yielded the respective esters as dark oils, with oleic acid producing 14.667 g (97.46%) and linoleic acid producing 14.402 g (96.19%). To assess the impact of solvents and catalysts, additional experiments were conducted using toluene and acetonitrile as solvents, while H<sub>2</sub>SO<sub>4</sub> and HCl were tested as catalysts under the same reaction conditions.

# Fourier transform infrared (FTIR) analysis on OOC and iodine value (IV)

For the analysis of OOC and IV, 0.5 mL samples were collected at regular intervals during the epoxidation and alcoholysis reactions for a spectral analysis. The spectra were recorded using a smart iTR diamond ATR between 400-4000 cm<sup>-1</sup>.

In the OOC analysis, the oxirane functional group was analysed based on the absorption band in the spectrum region of 1432.0-1497.3 cm<sup>-1</sup> with baselines defined between 762.2-862.3 cm<sup>-1</sup>. As for the IV analysis, the double bond absorption was measured in the region of 3004.2-3017.5 cm<sup>-1</sup>, with baseline points set between 2500.4-3035.2 cm<sup>-1</sup>. The measured FTIR peak areas were converted into OOC and IV values. The maximum percentage of OOC (% OOC<sub>max</sub>) were calculated to represent the theoretical conversion of all double bonds in PO<sub>o</sub> into oxirane rings in EPO<sub>o</sub> using equation 1 [22, 23]:

% OOC<sub>max</sub> = 
$$\left[\frac{(IV_i/2A_i)}{100+(IV_i/2A_i)A_0}\right] \times A_o \times 100$$
 (1)

where  $A_o = 16.0$  g/mol (atomic weight of oxygen);  $A_i = 26.9$  g/mol (atomic weight of iodine);  $IV_i = 62$  (initial iodine value of  $PO_o$ ) [24].

The loss of double bonds during epoxidation was calculated by equation 2:

% Loss of IV = 
$$\left(\frac{\Delta IV}{IV_i}\right) \times 100$$
 (2)

where  $\Delta IV = FTIR$  measured iodine value.

The percentage of epoxide yield was determined using equation 3:

% Yield = 
$$\left(\frac{FTIR\ OOC}{\%OOC\ max}\right) \times 100$$
 (3)

where FTIR OOC was the oxirane oxygen content measured at 1432-1497 cm<sup>-1</sup>.

During epoxidation, there is a slight change in IV, represented by  $\Delta IV$  due to the incorporation of oxygen into the oxirane rings, which increases the oil's total mass. This increase affects the IV calculation,

necessitating a correction ( $\Delta IV_{corrected}$ ) using equations 4 and 5 [23]:

% Mass increase = 
$$100/$$
 [(100 - FTIR (4) OOC%)-1] ×100

$$\Delta IV_{Corrected} = IV_i - \{[(IV_i - \Delta IV) \times \% \text{ mass } (5) \text{ increase}]/100\}$$

where  $IV_i$ = Initial iodine value and  $\Delta IV$ = FTIR measured iodine value.

# Characterisation analysis by FTIR and nuclear magnetic resonance (NMR)

The sample was analysed using FTIR spectroscopy within the frequency range of 400-4000 cm $^{\text{-}1}$ . The spectra were processed using the OMNIC software to identify and characterise the functional groups present in the sample. Further structural identification and characterisation were performed using Proton ( $^{1}\text{H}$ ) and Carbon ( $^{13}\text{C}$ ) NMR spectroscopy. The sample was diluted with 600  $\mu\text{L}$  of CDCl $_{3}$  in an NMR tube. The prepared tube was placed between the poles of the NMR magnet probe and irradiated with energy to obtain the spectra. The NMR spectra were recorded on a JEOL JNM-ECP 400 spectrometer, operating at 400.13 MHz for  $^{1}\text{H}\text{-NMR}$  and 100.77 MHz for  $^{13}\text{C}\text{-NMR}$ .

#### Acid value (AV) measurement

The AV test was conducted in accordance with the ISO 660:1996 procedure to determine the free fatty acids content in 1 g of fat. A 2.0 g sample was mixed with 50 mL of ethanol in an Erlenmeyer flask and heated to 75-80°C on a heating mantle for 1 hour. Following heating, two drops of phenolphthalein were added to the mixture which was then agitated vigorously. to the solution was titrated with 0.1 N potassium hydroxide (KOH) solution until a pale pink endpoint was achieved and maintained for at least 15 seconds. The AV test was performed in triplicate and the AV was calculated using equation 6 [25]:

$$AV = \frac{T \times N \times 56.1}{W} \tag{6}$$

where T= volume of KOH (mL), N= normality of standard KOH solution, W= weight of the sample (g).

# Saponification value (SV) measurement

The SV measurement was conducted according to the ASTM D464 procedure. A 2.0 g oil sample was dissolved thoroughly in 25 mL of 0.5 ethanolic KOH in an Erlenmeyer flask and then heated on a hot plate at 70°C for 1 hour. After heating, 2 drops of 1% phenolphthalein were added to the mixture to produce a pale pink colour. The mixture was immediately titrated with 0.5 N H<sub>2</sub>SO<sub>4</sub> until the solution became colourless. To minimise variability in test results,

titration was performed rapidly while the sample remained warm (60-70°C). The SV analysis was performed in triplicate for both the blank and the samples. The SV was calculated using equation 7 [25]:

$$SV = [(A-B) \times N \times 56.1] / W$$
 (7)

where  $A=H_2SO_4$  (mL) required for the blank titration,  $B=H_2SO_4$  (mL) used for the titration of samples, W= weight of the sample (g), N= normality of  $H_2SO_4$ . The SV was reported to the nearest whole number.

# Ester value (EV) measurement

The EV was determined as the amount of KOH (mg) required to react with the ester content of in 1 g of the sample following the saponification reaction. The EV was calculated as the difference between SV and AV with equation 8 [7]:

$$EV = SV - AV \tag{8}$$

where SV= saponification value and AV= acid value

#### Ester (EV) percentage

The ester percentage (%) was determined by equation 9.

where EV= ester value, MW= molecular weight of ester of 126.11 g/mol [7].

# Pour point (PP) value measurement

The pour point of sample was determined according to the standard procedure of American Society for testing Materials (ASTM D 97-05) with slight modifications [26]. The experimental setup is illustrated in Figure 1. The sample was filled into a test jar up to the 5.4 cm level mark. Then, the test jar was immersed in three different cooling baths, each maintaining specific temperatures. For 0°C, a mixture of 100 g crushed ice and 100 g water was used. To attain -12°C, 100 g of crushed ice was combined with 33 g of sodium chloride (NaCl) crystals. For the lowest temperature of -27°C, 100 g of crushed ice was mixed with 41 g of calcium chloride (CaCl<sub>2</sub>) crystals [33]. The temperature drop of the sample was monitored at 3°C intervals using a thermometer. After each temperature check, the sample was titled horizontally for 5 seconds, and the temperature was recorded when the sample no longer flowed. The procedure was repeated in triplicate, and the average temperature was recorded. An additional 3°C was added to the average value to determine the final PP [27].

# Results and Discussion **Epoxidation**

It was planned to react an organic peroxy acid (performic acid) with palm olein in a single-step mechanism as illustrated in Figure 2. It involves an oxygen transferred from performic acid to alkene in a cyclic to give an epoxide [28]. There is a transition state which shows how the bond breaking and new bond formation during epoxidation reaction [13]. In this reaction, the epoxidation progress was tracked continuously and monitored by the OOC and IV via the simple and rapid ATR-FTIR method. The parameters of OOC and IV represent the formation of oxirane groups and the loss of double bonds. IV indicates the number of double bonds while the OOC displays the percentage of epoxy content. The %OOC<sub>max</sub> for all the double bonds in the PO<sub>o</sub> to be converted into the oxirane ring was 3.76% which calculated from the equation 1. Based on Figure 3, the highest OOC content was achieved at 3.69%, the closest to the %OOC calculated max of 3.76%, which was obtained during reaction at 40°C for 153 min. This finding was consistent to Nor et al. [15]. There was a slow increase of OOC trend by conducting the reaction at low temperature (30°C) by contributing only a low OOC% of 2.62% which was 69.68% of epoxy conversion. This slow epoxidation rate resulted most probably due to limited activation energy that required more reaction time to increase the epoxy conversion [27]. In this study, the highest temperature was 60°C in which it reached its maximum experimental OOC% of 3.42% for 60 min of reaction, then dropped obviously to 2.89% at 153 min. This seems to suggest that after 60 min, the temperature had surpassed its equilibrium limit since the epoxidation was a reversible reaction [15]. In addition, the high temperature resulted in less epoxy content due to oxirane cleavage as it expected to undergo partial hydrolysis causing some of the epoxy groups to degrade [16]. To have a good quality of EPO<sub>0</sub>, the OOC% should be as high as possible, while the IV should be very low after the epoxidation.

The initial IV of PO<sub>o</sub> was 62 mg/g. During the epoxidation process, the IV value of sample progressively decreased due to the loss of double bonds. The lowest IV recorded was 9.5 mg/g, as measured by the small peak area at a frequency of 3009.86 cm<sup>-1</sup> with an absorbance unit (a.u.) of 0.08 in the FTIR spectrum. This substantial reduction in IV corresponded to a significant double-bond loss of 84.68%, indicating that nearly all the double bonds in PO<sub>o</sub> had successfully converted into the epoxy groups, with only a minimal percentage remaining in EPO<sub>o</sub>. In this study, the highest epoxide yield obtained was 90.65% by carrying the reaction at 40°C for 2.55 h in which considered as optimum condition for epoxidation. On the contrary, by running the reaction

at other temperatures (30°C, 35°C, 45°C, 50°C, 55°C, and 60°C) could only give epoxy yields of 62.03%,

82.40%, 87.13%, 71.37%, 67.82%, and 60.51% respectively.

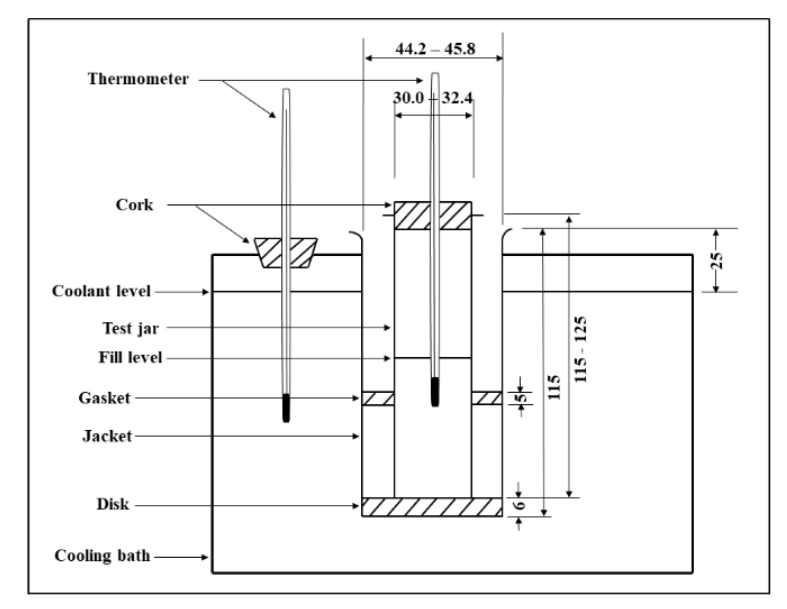


Figure 1. Experimental setup of pour point (PP) test

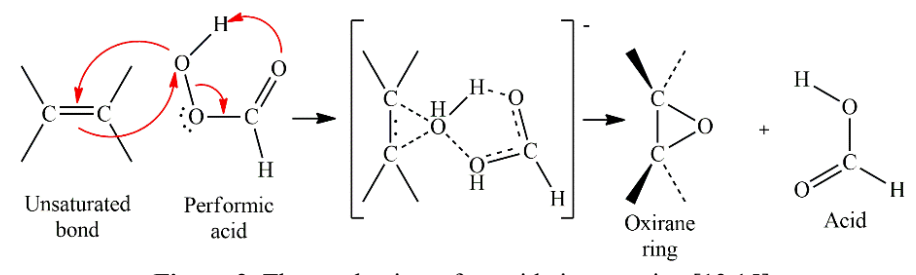


Figure 2. The mechanism of epoxidation reaction [13,15]

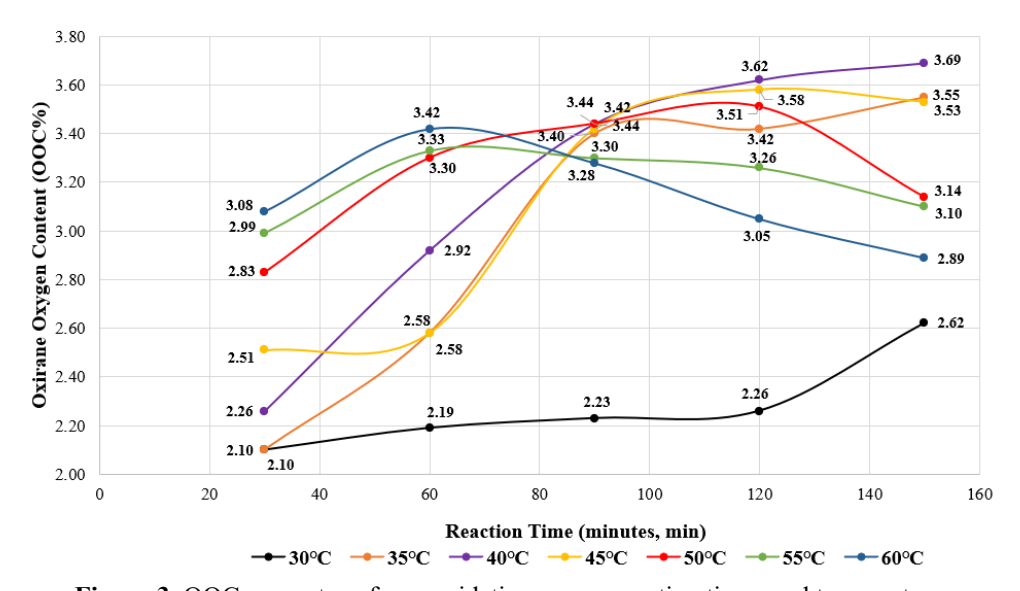


Figure 3. OOC percentage for epoxidation versus reaction times and temperatures

# Alcoholysis

An attempt at epoxide ring-opening was initiated by protonation using a Lewis acid (BF<sub>3</sub>·Et<sub>2</sub>O), a homogeneous catalyst to produce a protonated epoxide (Figure 3) [23]. The protonated epoxide then reacts with the glycerol to form a protonated polyol, which then transfer a proton to a molecule of water to give the polyols (hydroxyl-ether-PO<sub>0</sub>) and a hydronium ion. In this step, the epoxide ring-opening was monitored based on reduction of OOC% over the time at different temperatures as shown in Figures 4 and 5. Based on the analysis, the optimum temperature for the alcoholysis was discovered at 120°C for the duration of 4 h. Under this condition, the lowest OOC% of 0.28% with a high conversion to polyols of 92.45% and reaction yield of 85.93% was obtained. In general, the lower OOC% indicates the higher loss of oxirane rings due to ring-opening reaction suggesting more introduction of hydroxyl groups into the desired intermediate. At 120°C, the trend of OOC% was decreasing significantly from 2.34% to 0.28% up to 4 h of reaction before started developing again and stayed at the constant value of 1.35%. This indicated that it had reached its equilibrium at 4 h but it became reversible beyond 4 h due to the limiting amount of reactant.

However, treatment at low temperature of 90°C showed the poorest ring-opening performance. Its OOC value was decreasing slowly each hour beginning with the highest OOC% of 3.34% during the first hour and slowly decreased to 3.12% (2 h), 3.05% (3 h), 3.05% (4 h), 2.63% (5 h), and 1.92% (6 h). At the end of the ring-opening reaction (after 6 h), the OOC% for the temperature of 90°C, 100°C, and 110°C were 1.92%, 1.28%, and 0.78% respectively signifying the presence of remaining oxirane rings in the EPO<sub>o</sub> even after longer reaction time below 120°C. Additionally, it was observed that treatment up to 120°C demonstrated a better conversion due to deactivation of BF<sub>3</sub>·Et<sub>2</sub>O catalyst above 120°C.

Furthermore, its boiling point was 130°C so the evaporation, decomposition, and the loss of catalytic activity may occur. Thus, the reaction temperature higher than 120°C was not recommended in this experimental setup.

#### **Esterification mechanism**

For the final esterification step, we considered oleic acid, linoleic acid, and salicylic acid as condensing agents by reacting it with polyol to give oleic acid-esterified-PO<sub>0</sub> (OA-EPO), linoleic acid-esterified-PO<sub>0</sub> (SA-EPO). The reaction mechanism between polyols intermediate and different type of acids via Fischer esterification is proposed as illustrated in **Figure 6**. In this reaction, the OH groups of polyols convert into ester (C=O) groups which will further broaden the mid-chain length between triglycerides of palm olein.

The initial step involves the protonation of carboxylic acid when carboxyl oxygen accepting a proton from the strong acid catalyst of H<sub>2</sub>SO<sub>4</sub> to form an oxonium ion. The carbonyl's carbon atom becomes more electrophilic because there is a partial positive charge on the electronegative oxygen atom. The second step involves the attack of the nucleophile from hydroxylether-POo on the carbonyl group to give a tetrahedral intermediate. One of the hydroxyl groups receives the proton to form a good leaving group (+OH<sub>2</sub>). This step forms an unstable tetrahedral intermediate which needs a further rearrangement. Hence, in a step 3, the loss of water molecule occurs to give a protonated ester. It is then followed by a proton transfer to Lewis base from protonated ester that will lead to a desired product of an ester. In the reaction, the catalyst is regenerated, and its surface is available for the next catalytic cycle. This mechanism is consistent to Ahmed et al. stressing that the nucleophilic substitution step of the esterification reaction is slow since the pi-bond is difficult to break although the rate of proton donating step is rapid (Step 1) [28, 29].

# Step 1: Protonation on oxirane ring to produce a protonated epoxide

Oxirane ring
Step 2: The protonated epoxide reacts with glycerol to form a protonated polyol

Step 3: Deprotonation to form the polyol and a hydronium ion

Figure 4. The mechanism of alcoholysis reaction [23]

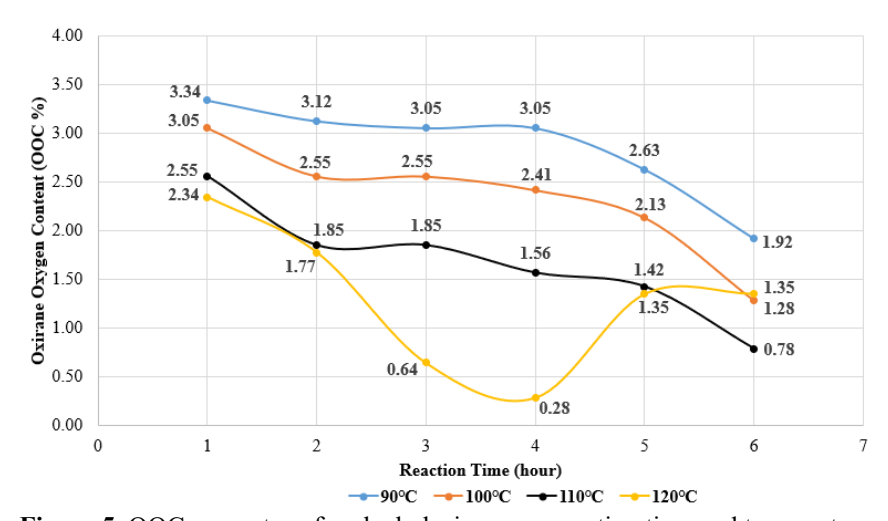


Figure 5. OOC percentage for alcoholysis versus reaction time and temperatures

Figure 6. A proposed mechanism of Fischer esterification reaction of polyols derived from palm olein [28].

# Optimisation of esterification reaction

In this study, several variables were used to optimize the esterification reaction including reaction temperatures, duration of reaction, types of solvents, types of reactants, and different acid catalysts. Based on the analysis, there was a significant increase in reaction yield and ester values by increasing the temperature from 90°C up to 140°C for 4 h of reaction (**Table 1**). This might be because esterification reaction is generally reversible so more activation energy from the heat can improve the reaction rate to achieve the equilibrium state and shift the position of equilibrium forward by adding amount of ester formed in which molecules easier entering the inner pore of catalyst [30].

However, increasing the temperature to 150 °C is not recommended because it would not only fasten the reaction rate but also lead to even higher risk of undesirable side reactions like oxidation [31]. The best reaction yield was 99.29% with the ester value of 93.61% highlighting the reaction catalysed by H<sub>2</sub>SO<sub>4</sub> in the organic solvent of toluene at 140°C. Using the solvent of acetonitrile in the presence of H<sub>2</sub>SO<sub>4</sub>, the highest ester value was achieved at 97.04 % with the ester yield of 98.71%. In this transformation, the esterification equilibrium was promoted by the solvents due to the liquid-phase reaction environment

that could speed up the catalyst utilization and contributed to a greater solubility of samples. In addition, the catalyst of H<sub>2</sub>SO<sub>4</sub> was more preferred than HCl due to higher boiling point in which suitable for optimum esterification reaction that required higher temperature (140°C). The presence of strong acid catalysts also enhanced the rate of esterification reaction. In the absence of strong acids catalyst, this Fischer esterification proceed very slowly.

By considering all parameters taken, treatment at 140 °C for the duration of 4 h by using hydrophobic solvent of toluene, and the catalyst of H<sub>2</sub>SO<sub>4</sub> were chosen as the optimal conditions for esterification reaction in the synthesis of esterified palm olein. On top of that, the oleic acid-esterified palm olein (OA-EPO) gave the highest ester values of 96.79% followed by the salicylic acid-esterified palm olein (SA-EPO) with 93.61% and the linoleic acidesterified palm olein (LA-EPO) of 92.86%. Apart from the ester values, the ester products which gained the best reaction yield was the SA-EPO with 99.29% which was higher than OA-EPO of 97.46% and LA-EPO of 96.19%. Overall, oleic acid, salicylic acid and linoleic acid gave excellent ester value (92.86-96.79%) and percentage yield (96.19-99.29%) during esterification reaction.

Malays. J. Anal. Sci. Volume 29 Number 3 (2025): 1404

Table 1. Optimisation of esterification reaction using salicylic acid

Run order	Temperature (°C)	Solvent	Catalyst	Reaction Yield (%)	Ester Value (%)
1	90	Toluene	H <sub>2</sub> SO <sub>4</sub>	40.20	74.22
2	90	Acetonitrile	$H_2SO_4$	42.93	61.47
3	90	Toluene	HCl	41.73	72.51
4	90	Acetonitrile	HCl	31.82	63.17
5	120	Toluene	$H_2SO_4$	71.58	63.19
6	120	Acetonitrile	$H_2SO_4$	72.07	64.47
7	120	Toluene	HCl	75.12	78.25
8	120	Acetonitrile	HCl	77.78	84.37
9	140	Toluene	$H_2SO_4$	99.29	93.61
10	140	Acetonitrile	$H_2SO_4$	98.71	97.04
11	140	Toluene	HCl	80.42	92.17
12	140	Acetonitrile	HCl	82.80	87.57

# Characterisation analysis by FTIR and NMR Epoxidation

FTIR analysis was performed to analyse and identify the chemical bonds as well as functional groups in the samples. Spectra of natural POo and EPOo were compared in Figure 7. Two small peaks observed at the frequency of 3009.86 cm<sup>-1</sup> and 1655.88 cm<sup>-1</sup> represented unsaturated double bonds in the fatty acid composition of raw sample of PO<sub>0</sub>. The appearance of a new peak at 836.94 cm<sup>-1</sup> in EPO<sub>o</sub> spectrum showed the existence of epoxide group (C-O-C). At the same time, the small peaks for unsaturated double bonds at 3009.86 cm<sup>-1</sup> and 1655.88 cm<sup>-1</sup> had disappeared [14,15]. This confirmed the transformation of double bonds into the oxirane rings during the epoxidation. This result was consistent to Jalil et al. [14] confirming the epoxide group was observed in the frequency range between 815 cm<sup>-1</sup> to 950 cm<sup>-1</sup>. Both FTIR spectra also consist of stretching peaks at approximately 2852 cm<sup>-1</sup> and 2921 cm<sup>-1</sup> which were methyl CH2 and CH3 stretching vibration as well as the bending vibration of CH<sub>2</sub> at 1462 cm<sup>-1</sup>. Meanwhile, the aliphatic chain with CH2 oscillatory vibration was located at 721 cm<sup>-1</sup>.

Apart from FTIR analysis, proton NMR (<sup>1</sup>H-NMR) and carbon NMR (<sup>13</sup>C-NMR) spectra were used to support the formation of epoxide during epoxidation reaction. To carry out the NMR analysis, the sample was dissolved in deuterated chloroform (CDCl<sub>3</sub>). The solvent peak appeared at the chemical shift of 7.25

ppm (<sup>1</sup>H-NMR spectrum) and between 76-77 ppm (13C-NMR spectrum). The 1H-NMR spectra of PO<sub>o</sub> and EPO<sub>o</sub> were shown in Figures 8 and 9, respectively. The presence of unsaturated double bonds (HC=CH) of natural POo can be seen at 5.30 ppm. The appearance of a new signal peak at 2.85 ppm in the EPO<sub>o</sub> spectrum indicated the successful formation of epoxide groups (H-C-O-C-H) in which corroborated by earlier finding [19] revealing the epoxide ring were seen at 2.88 ppm. After the epoxidation, both of the peaks of olefin proton (C=C-H) at 5.30 ppm and its allylic proton (C=C-C-H) at 2.01 ppm in the POo had disappeared and replaced by the oxirane ring peak signal (H-C-O-C-H) at 2.85 ppm and the epoxy proton (CH<sub>2</sub>-CHOCH-CH<sub>2</sub>) at 1.44 ppm. The disappearance of the peak area for the double bonds with 13.336 a.u. but the presence of oxirane ring with 11.359 a.u. had evidenced the successful of epoxidation reaction. Furthermore, the signals of long aliphatic chain (CH<sub>2</sub>) and the terminal CH3 were shown in both spectra at 1.22 ppm (peak 2) and 0.84 ppm (peak 1) respectively. Figure 10 displayed the <sup>13</sup>C-NMR analysis of PO<sub>o</sub> and EPOo, respectively. In POo spectrum, the peaks of unsaturated double bonds (C=C) were shown at the chemical shift from 127 to 130 ppm. The conversion of double bonds into the oxirane rings during the epoxidation process was supported by the appearance of new peaks at 54 to 57 ppm in which represented the oxirane ring (C-O-C) and the absence of alkene peaks (127-130 ppm).

Malays. J. Anal. Sci. Volume 29 Number 3 (2025): 1404

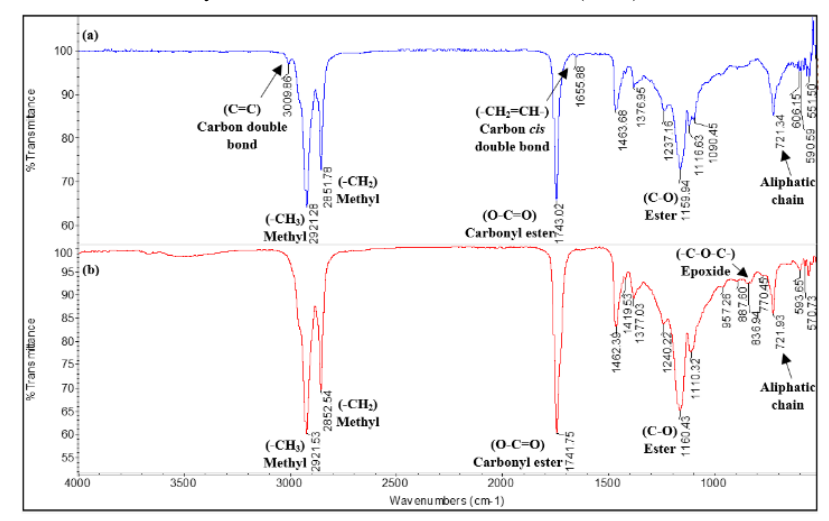


Figure 7. Comparative FTIR spectra of  $PO_o\left(a\right)$  and  $EPO_o\left(b\right)$ 

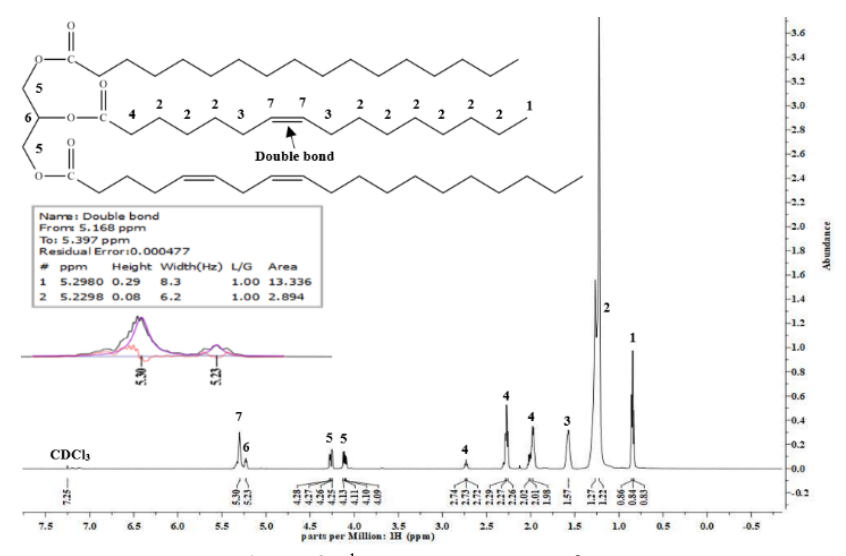


Figure 8. <sup>1</sup>H-NMR spectrum of PO<sub>o</sub>

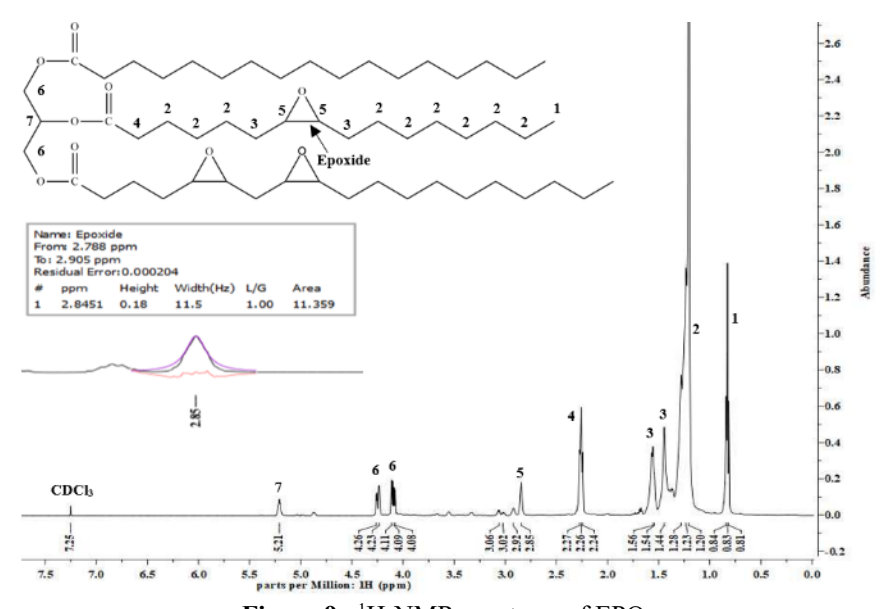


Figure 9.  $^{1}\text{H-NMR}$  spectrum of EPO $_{o}$ 

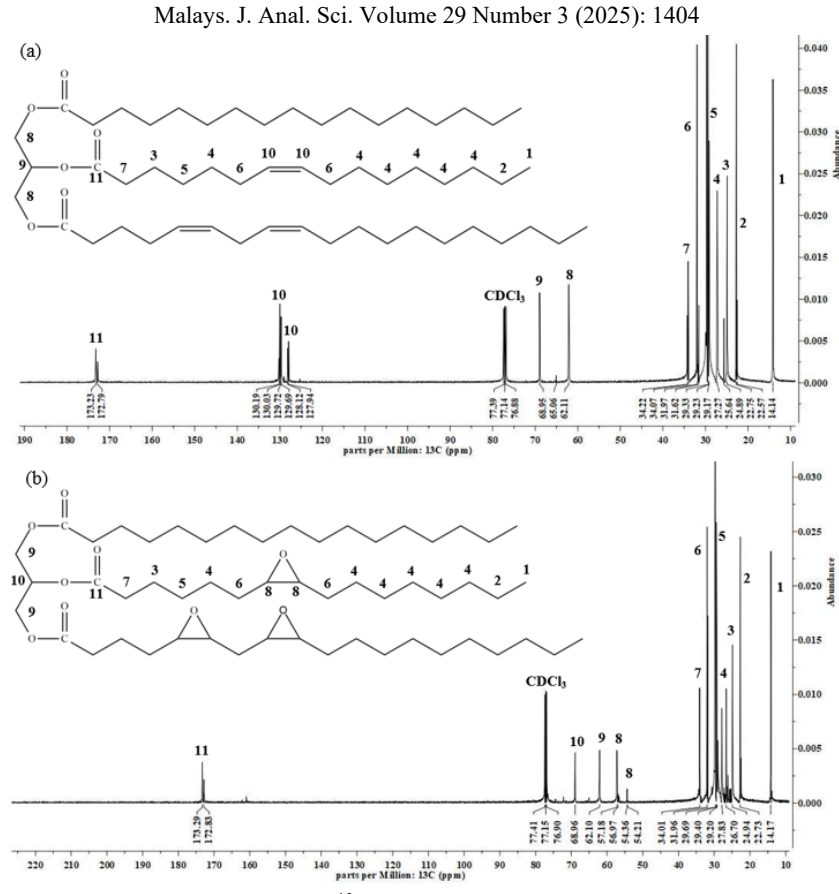


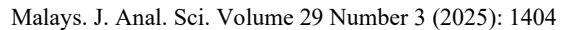
Figure 10. Comparative <sup>13</sup>C-NMR spectra of PO<sub>o</sub> (a) and EPO<sub>o</sub> (b)

#### Alcoholysis

The appearance of a new broad band in the FTIR spectrum between 3300 to 3650 cm<sup>-1</sup> assigned to the stretching vibrations of hydroxyl (O-H) groups suggested that the ring opening had occurred (Figure 11). The regions between 1000 and 1300 cm<sup>-1</sup> were the absorption peaks for ether group [23, 34]. The absence of epoxy group peak at 836.94 cm<sup>-1</sup> provides more support on the conversion of EPOo to polyols. The peak area (a.u.) of OH groups synthesized in the first hour was 437.28 continued to expand by the following second hours (466.23), third hours (698.81), and the highest at the fourth hours (766.99). Then, it started to diminish in the reaction time of five hours (543.16) and six hours (523.30). In view of this, the ringopening reaction was greatly influenced by both reaction temperature and reaction time. To sum up, the optimal experimental conditions of the ring opening reaction using glycerol was 4 hours at reaction temperature of 120°C.

As indicated in the <sup>1</sup>H-NMR spectrum (**Figure 12**), the oxirane ring opening was further supported by the

formation of new peaks at regions from 3.34 to 3.89 ppm corresponding to OH and ether groups. The spectrum confirmed the disappearance of the epoxy group in the structure due to the absence of peak at 2.85 ppm indicating the oxirane ring has been opened successfully from alcoholysis reaction. This finding was consistent to the reference [23] that the appearance of a new signal peak at 2.66 ppm in the spectrum indicated the successful formation of OH groups. Based on <sup>13</sup>C-NMR spectrum, two missing peaks observed at 54 to 57 ppm for the epoxy groups explained the successful conversion to polyols. This was supported by the appearance of the new peaks at 70.18 to 74.38 ppm for OH group and at 68.96 ppm for the ether group. The result of carbon NMR analysis agreed with the data from proton NMR and FTIR spectra analysis. From these experiments, hydroxyl-ether-PO<sub>o</sub> (polyols) was successfully prepared via alcoholysis reaction using glycerol at 85.93% yield which allowed more incorporation of the hydroxyl groups into the structure prior to esterification reaction.



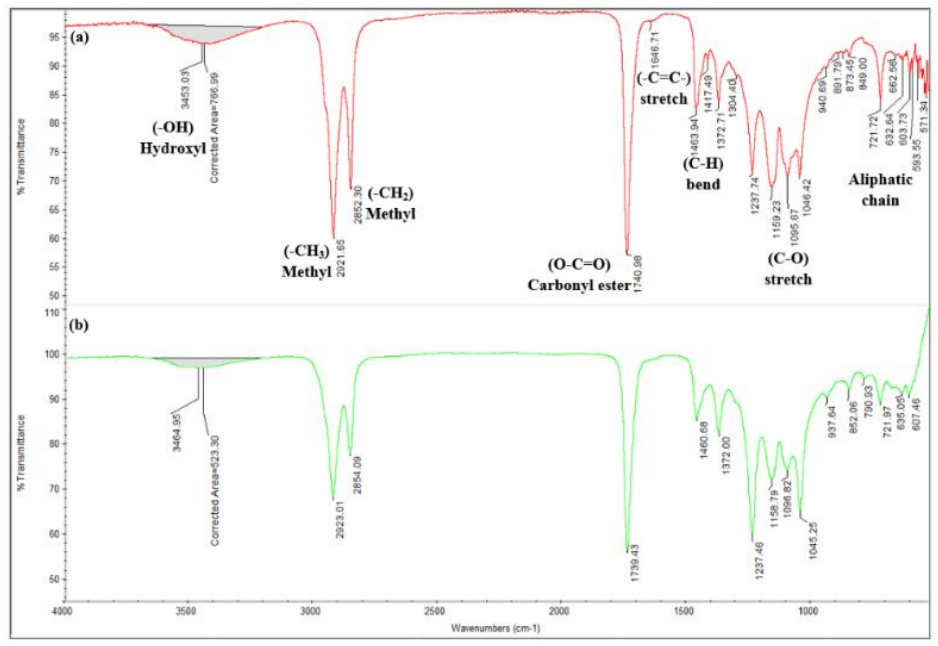


Figure 11. Comparative FTIR spectra of hydroxyl-ether-PO<sub>o</sub> in 4 h (a) and 6 h (b) of reaction

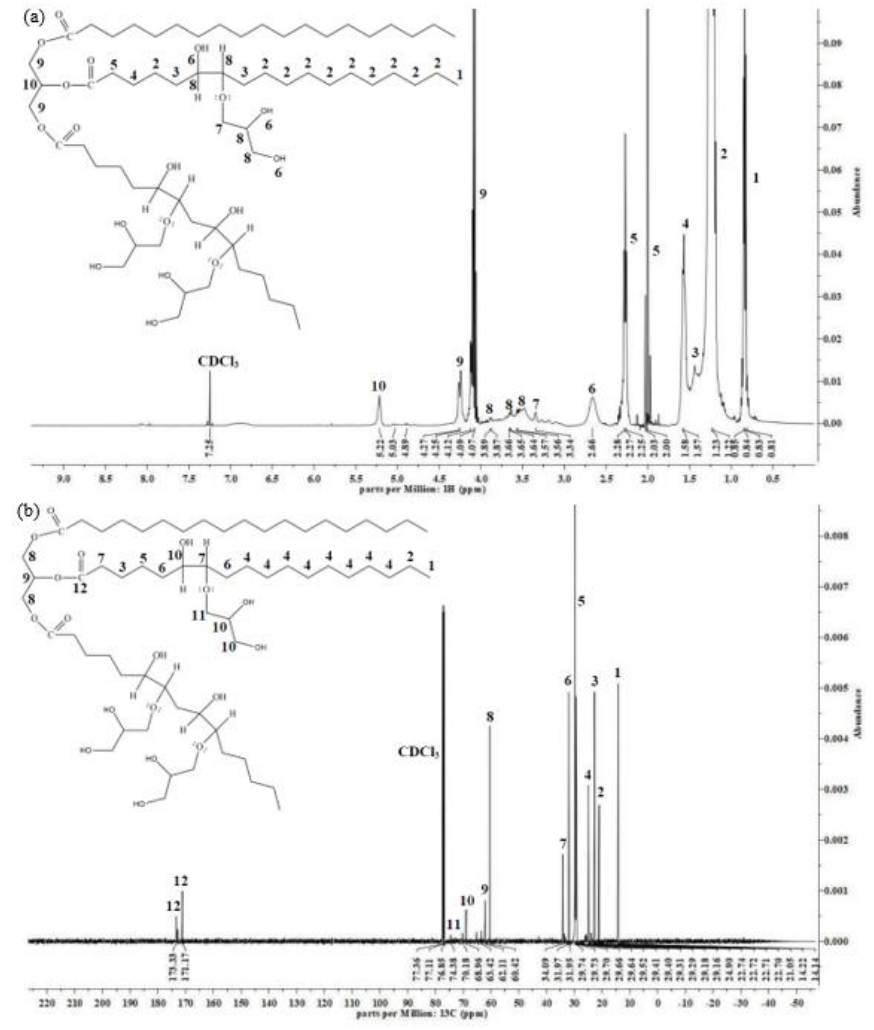


Figure 12.  $^{1}\text{H-NMR}$  (a) spectrum and  $^{13}\text{C-NMR}$  (b) spectrum of hydroxyl-ether-PO $_{o}$ 

#### **Esterification**

The FTIR spectra of LA-EPO, OA-EPO, and SA-EPO were illustrated in **Figure 13**. Both FTIR spectra of LA-EPO and OA-EPO shared a common characteristic where the broad OH absorption bands that ranged between 3200 to 3650 cm<sup>-1</sup> had disappeared indicating the successful conversion of OH groups to esters. These conversions were supported by the appearance of intense peaks of C=O esters at 1739.65 cm<sup>-1</sup> (LA-EPO) and 1740.64 cm<sup>-1</sup> (OA-EPO) concurrently with the C-O ester stretching peak at around 1162.41 cm<sup>-1</sup> (LA-EPO) and 1160.27 cm<sup>-1</sup> (OA-EPO). The small peak observed at 1672.82

cm<sup>-1</sup> (LA-EPO) and 1628.50 cm<sup>-1</sup> (OA-EPO) were contributed from the unsaturated double bonds in the fatty acid composition of the linoleic and oleic acid. This characterization was consistent to the literature of C=O ester peak (1740 cm<sup>-1</sup>) and C-O esters (1000 to 1300 cm<sup>-1</sup>) [31]. SA-EPO displayed the C-O ester peaks from 1156.04 to 1240.34 cm<sup>-1</sup>, unsaturated  $\alpha,\beta$  C=O ester compounds at 1678.39 to 1710.82 cm<sup>-1</sup>, and the carbonyl stretching C=O ester peak at 1737.60 cm<sup>-1</sup> [35]. From the FTIR analysis, the ester functionalities had been observed in all the esterified palm olein of LA-EPO, OA-EPO, and SA-EPO.

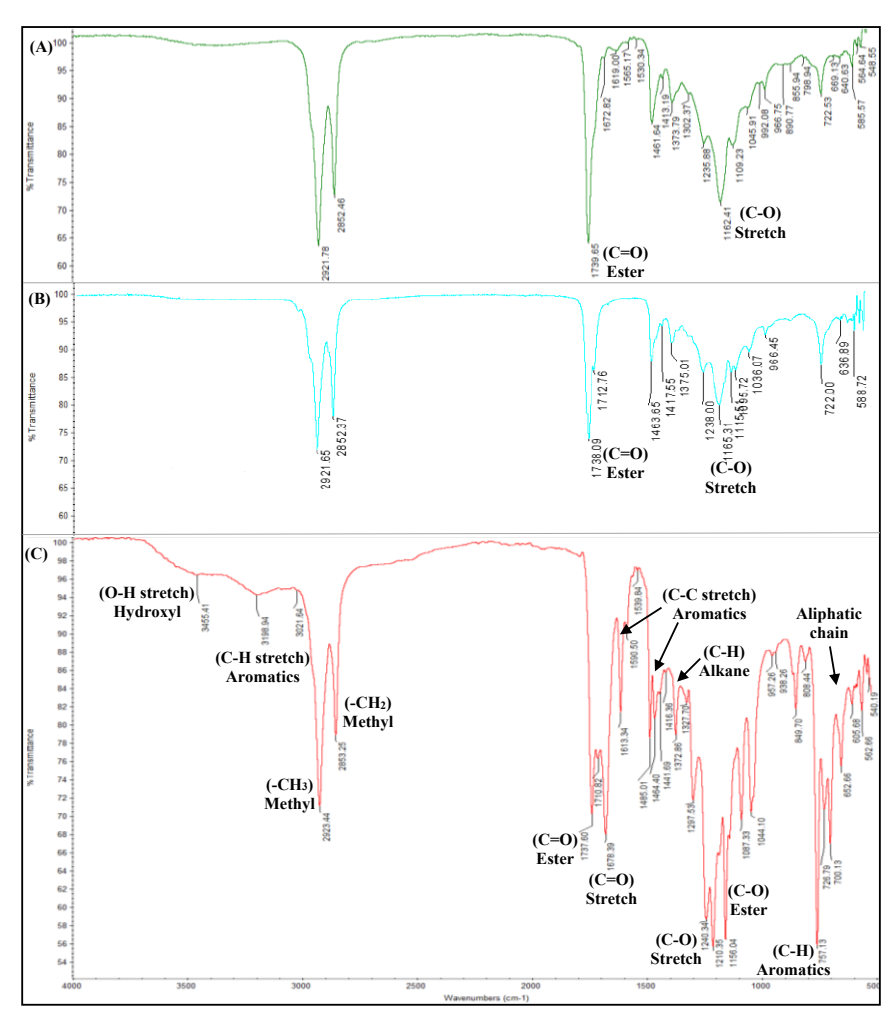


Figure 13. FTIR spectra of LA-EPO (A), OA-EPO (B), and SA-EPO (C).

<sup>1</sup>H-NMR spectrum of SA-EPO showed the presence of ester (RCOO-CH) peaks between 4.1 ppm and 4.3 ppm, HC-COOR (2.0-2.3 ppm), and the ether (HC-OR) at 3.93 ppm (**Figure 14**). The hydroxyl substituent on the aromatic rings resonated at 5.38 ppm while the aromatic C-H appeared in the regions from 6.83 ppm to 6.93 ppm and between 7.42ppm to 7.76 ppm. This was further supported by <sup>13</sup>C-NMR spectrum by the appearance of new peaks at 171 ppm

and 173 ppm due to the presence of ester (C=O) groups (**Figure 15**). The carbon next to the ester (R-CH<sub>2</sub>-C=O) was figured at 34 ppm and the appearance of resonance at 117.73 ppm and 129.92 ppm could be assigned to benzene ring carbons. Based on several spectra evidence of SA-EPO, polyols derived from palm olein was successfully esterified using salicylic acid to install large-branched esters between triglycerides throughout the esterification reaction.

#### **Pour Point test**

Pour point (PP) is critical performance metric for petroleum-based products, indicating the lowest temperature at which the fluid movement is observed. More unsaturation and shorter carbon chains generally result in lower PP values [32]. One of the drawbacks of natural PO<sub>0</sub> is its high PP value of 6°C, limiting its application as a lubricant at low temperature environments due to its tendency to solidify. Following epoxidation, the PP of PO<sub>0</sub> improved from 6°C to -1°C, indicating enhanced cold flow properties. However, after the ring-opening reaction, the PP increased to 5°C. This reduction in cold flow efficiency could be attributed to the introduction of branched chains and hydroxyl groups, which hindered molecular packing and increase the tendency toward crystallisation at low temperatures. Despite these modifications, the issue of poor cold flow properties

persisted, necessitating the esterification process for further enhancement. The OH group played a vital role in the esterification reaction by engaging in structural modifications that introduced largebranched ester groups. These groups disrupted the molecular symmetry and spatial arrangement, creating a steric hindrance that delayed the crystallisation process to improve cold flow properties. Among the esterified products, SA-EPO demonstrated the best low-temperature performance, achieving a PP of -12°C, compared to -7°C for OA-EPO and -11°C for LA-EPO (Table 2). Based on the findings presented in Table 2, these improvements highlighted the effectiveness in incorporating large-branched esters in mitigating the self-stacking tendencies of triglycerides in natural POo, preventing the formation of macrocrystalline structures down to -12°C.

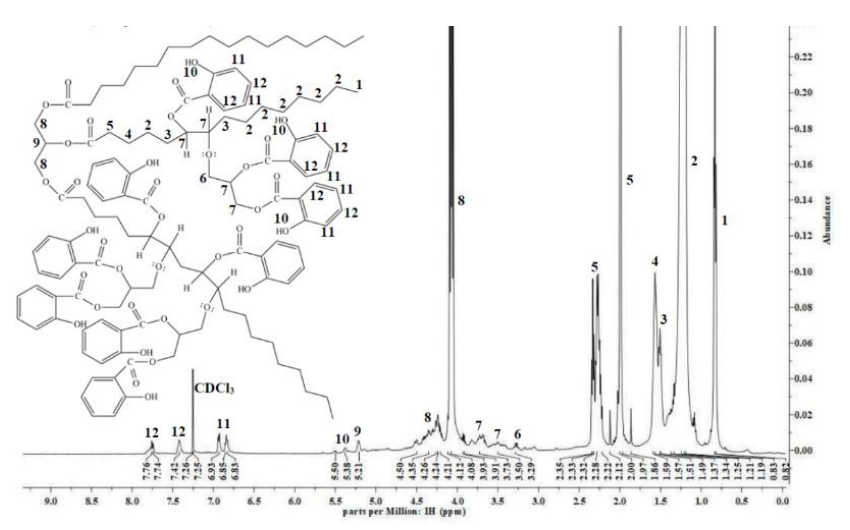


Figure 14. <sup>1</sup>H-NMR spectrum of SA-EPO

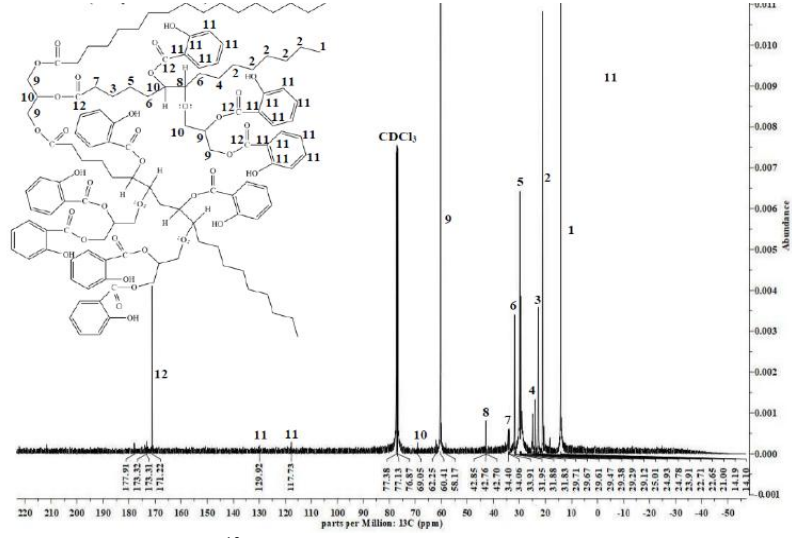


Figure 15. <sup>13</sup>C-NMR spectrum of SA-EPO

**Table 2.** The AV, SV and EV values of raw sample, intermediates and esterified products

	PO <sub>0</sub>	EPO <sub>o</sub>	Hydroxyl-ether-	OA-EPO	LA-EPO	SA-EPO
			POo			
Yield (%)	-	$90.65 \pm 0.00$	$85.93 \pm 0.00$	$97.46 \pm 0.00$	$96.19 \pm 0.00$	$99.29 \pm 0.00$
OOC value (%)	0	$3.69 \pm 0.00$	$0.28 \pm 0.00$	-	-	-
Conversion (%)	-	$98.14 \pm 0.00$	$92.45\pm0.00$	-	-	-
Iodine value	$62 \pm 0.00$	$9.5{\pm}~0.01$	-	-	-	-
Acid value (mg KOH/g)	$10\pm0.94$	$32\pm0.94$	$13 \pm 2.47$	$12\pm1.00$	$3\pm0.77$	8 ± 1.48
Saponification value (mg KOH/g)	$154 \pm 3.28$	$153\pm1.53$	$159 \pm 2.22$	$443 \pm 20.68$	$416\pm1.17$	$424 \pm 21.90$
Ester value (mg KOH/g)	$144 \pm 4.06$	$121 \pm 2.52$	$146 \pm 4.41$	$431 \pm 21.28$	$413\pm1.45$	$416\pm20.76$
Ester value (%)	$32.38 \pm 0.91$	$27.25\pm0.57$	$32.90 \pm 0.99$	$96.79 \pm 4.78$	$92.86 \pm 0.33$	$93.61 \pm 4.67$
Pour point (°C)	$6 \pm 0.58$	$-1 \pm 0.00$	$5 \pm 0.58$	$-7 \pm 0.88$	$-11 \pm 0.33$	$-12 \pm 0.33$

#### Conclusion

This research study focused on the synthesis of green lubricant by chemically modifying the structure of palm olein via three main processes which were epoxidation, alcoholysis, and the esterification reactions. The ideal reaction temperature and time was achieved at 140°C for the duration of 4 h to prepare the esterified palm olein of OA-EPO, LA-EPO, and SA-EPO at 97.46%, 96.19%, and 99.29% of yield, respectively. In the pour point test, all large-branched esterified palm olein showed significant cold flow improvement particularly SA-EPO and LA-EPO with the PP value of -12°C and -11°C, respectively which was better than OA-EPO (-7°C) relative to the natural palm olein with a poor cold flow behaviour of 6°C. Overall, the findings from this study suggested largebranched esterified palm olein prepared by extending the gap between triglycerides molecules could reduce the pour point values up to -12°C highlighting their potentials as a source of green lubricant. For further study, continuous research on esterified palm olein of OA-EPO, LA-EPO, and SA-EPO in the field of green chemistry is strongly recommended to produce valueadded green lubricating products. The esterified palm olein comprising large-branched structure prepared in this study have great potential to be developed further as an alternative to mineral oil-based lubricants and convenient for large scale production.

### Acknowledgement

The authors would like to acknowledge the financial support and facilities provided from the Department of Chemistry, Faculty of Resource Science and Technology, University Malaysia Sarawak for this study. The authors would also like to express special appreciation to the Department of Mechanical and Manufacturing Engineering, Faculty of Engineering, University Malaysia Sarawak for their support in the pour point experimental setup.

### References

- 1. Nor, N. M., Salih, N., and Salimon, J. (2022). Optimization and lubrication properties of Malaysian crude palm oil fatty acids based neopentyl glycol diester green biolubricant. *Renewable Energy*, 200: 942-956.
- Pinheiro, C. T., Quina, M. J., and Gando-Ferreira, L. M. (2021). Management of waste lubricant oil in Europe: A circular economy approach. *Critical Reviews in Environmental Science and Technology*, 51(18): 2015-2050.
- 3. Lee, D. J., and Song, S. H. (2019). Investigation of epoxidized palm oils as green processing AIDS and activators in rubber composites. *International Journal of Polymer Science*, 2019 (42): 1-7.
- 4. Salih, N. (2021). A review on eco-friendly green biolubricants from renewable and sustainable plant oil sources. *Biointerface Research in Applied Chemistry*, 11(5): 13303-13327.
- 5. Voon, P. T., Lee, S. T., Ng, T. K. W., Ng, Y. T., Yong, X. S., Lee, V. K. M., and Ong, A. S. H. (2019). Intake of palm olein and lipid status in healthy adults: A meta-analysis. *Advances in Nutrition*, 10(4): 647-659.
- 6. Hambali, E., and Puspita, N. N. I. A. (2021). Epoxidation of palm olein as base oil for calcium complex bio grease. *International Journal of Oil Palm*, 4(1): 22-30.

- 7. Tajau, R., Rohani, R., and Salleh, M. Z. (2020). Physicochemical and thermal properties of acrylated palm olein as a promising biopolymer. *Journal of Polymers and the Environment*, 28 (10): 2734-2748.
- Abubakar, A., Ishak, M. Y., and Makmom, A. A. (2021). Impacts of and adaptation to climate change on the oil palm in Malaysia: A systematic review. *Environmental Science and Pollution Research*, 28: 54339-54361.
- 9. Yeong, S. P., Chan, Y. S., Law, M. C., and Ling, J. K. U. (2022). Improving cold flow properties of palm fatty acid distillate biodiesel through vacuum distillation. *Journal of Bioresources and Bioproducts*, 7(1): 43-51.
- 10. Dandan, A., and Samion, S. (2017). Palm oil as an alternative lubricant oil: A brief review. *The Colloquium*, *UTM*, 11: 17-19.
- Jalil, M. J., Yamin, A. F. M., Azmi, I. S., Jamaludin, S. K., and Daud, A. R. M. (2018). Mechanism and kinetics study in homogenous epoxidation of vegetable oil. *International Journal of Engineering & Technology*, 7: 124-126.
- Wu, Z., Zheng, T., Wu, L., Lou, H., Xie, Q., Lu, M., Zhang, L., Nie, Y., and Ji, J. (2017). Novel reactor for exothermic heterogeneous reaction systems: Intensification of mass and heat transfer and application to vegetable oil epoxidation. *Industrial and Engineering Chemistry Research*, 56(18): 5231-5238.
- Danov, S. M., Kazantsev, O. A., Esipovich, A. L., Belousov, A. S., Rogozhin, A. E., and Kanakov, E. A. (2017). Recent advances in the field of selective epoxidation of vegetable oils and their derivatives: A review and perspective. *Catalysis Science and Technology*, 7(17): 3659-3675.
- 14. Jalil, M. J., Rani, N. H. A., Yamin, A. F. M., Anuar, N. R. A., Azmi, I. S., and Hadi, A. (2019). Epoxidation reaction parameter of palm olein for synthesis of dihydrostearic acid (DHSA) via hydrolysis reaction. *IOP Conference Series:* Materials Science and Engineering, 551(1): 012001.
- 15. Nor, N. M., Derawi, D., and Salimon, J. (2018). The optimization of RBD palm oil epoxidation process using D-optimal design. *Sains Malaysiana*, 47(7): 1359-1367.
- 16. Yunus, M. Z. M., Jamaludin, S. K., Karim, S. F. A., Gani, A. A., and Sauki, A. (2018). Catalytic efficiency of titanium dioxide (TiO<sub>2</sub>) and zeolite ZSM-5 catalysts in the in-situ epoxidation of palm olein. *IOP Conference Series: Materials Science and Engineering*, 358(1): 012070.
- 17. Prociak, A., Malewska, E., Kurańska, M., Bąk, S., and Budny, P. (2018). Flexible polyurethane foams synthesized with palm oil-based biopolyols obtained with the use of different oxirane

- ring opener. *Industrial Crops and Products*, 115: 69-77.
- Uprety, B. K., Reddy, J. V., Dalli, S. S., and Rakshit, S. K. (2017). Utilization of microbial oil obtained from crude glycerol for the production of polyol and its subsequent conversion to polyurethane foams. *Bioresource Technology*, 235: 309-315.
- Noor, N. M., Ismail, T. N. M. T., Noor, M. A. M., Palam, K. D. P., Sattar, M. N., Hanzah, N. Ain, Adnan, S., and Kian, Y. S. (2022). Physicochemical properties of palm olein-based polyols prepared using homogeneous and heterogeneous catalysts. *Journal of Oil Palm Research*, 34(1): 167-176.
- 20. Ho, Y. H., Parthiban, A., Thian, M. C., Ban, Z. H., and Siwayanan, P. (2022). Acrylated biopolymers derived via epoxidation and subsequent acrylation of vegetable oils. *International Journal of Polymer Science*, 2022 (2): 1-12.
- Nor, N. M., and Salimon, J. (2023). Synthesis and characterization of palm oil pentaerythritol esterbased biolubricant from Malaysia palm oil. *Malaysian Journal of Analytical Sciences*, 27(4): 716-727.
- 22. Wai, P. T., Jiang, P., Shen, Y., Zhang, P., Gu, Q., and Leng, Y. (2019). Catalytic developments in the epoxidation of vegetable oils and the analysis methods of epoxidized products. *RSC Advances*, 9(65): 38119-38136.
- Tavassoli-Kafrani, M. H., Voort, F. R. V. D., and Curtis, J. M. (2017). The use of ATR-FTIR spectroscopy to measure changes in the oxirane content and iodine value of vegetable oils during epoxidation. *European Journal of Lipid Science* and Technology, 119(7): 1-11.
- Jurid, L. S., Zubairi, S. I., Kasim, Z. M., and Kadir, I. A. A. (2020). The effect of repetitive frying on physicochemical properties of refined, bleached and deodorized Malaysian Tenera palm olein during deep-fat frying. *Arabian Journal of Chemistry*, 13(7): 6149-6160.
- Nduka, J. K. C., Omozuwa, P. O., and Imanah, O. E. (2021). Effect of heating time on the physicochemical properties of selected vegetable oils. *Arabian Journal of Chemistry*, 14(4): 103063.
- Samidin, S., Salih, N., and Salimon, J. (2021). Synthesis and characterization of trimethylolpropane based esters as green biolubricant basestock. *Biointerface Research in Applied Chemistry*, 11(5): 13638-13651.
- 27. Yeong, S. P., Chan, Y. S., Law, M. C., and Ling, J. K. U. (2022). Improving cold flow properties of palm fatty acid distillate biodiesel through vacuum distillation. *Journal of Bioresources and Bioproducts*, 7(1): 43-51.

- 28. Solomons, T. W. G., Fryhle, C. B., and Snyder, S. A. (2014). *Organic Chemistry*, 11<sup>th</sup> edition. John Wiley & Sons, United States: pp. 789-791.
- Ahmed, R. A., Rashid, S., and Huddersman, K. (2023). Esterification of stearic acid using novel protonated and crosslinked amidoximated polyacrylonitrile ion exchange fibres. *Journal of Industrial and Engineering Chemistry*, 119: 550-573.
- Xu, J., Kong, L., Deng, L., Mazza, G., Wang, F., Baeyens, J., and Nie, K. (2021). The conversion of linoleic acid into hydroxytetrahydrofuranstructured bio-lubricant. *Journal of Environmental Management*, 291: 112692.
- 31. Kopchev, V. P., and Bayryamov, S. G. (2022). Study on the most important factors for the optimization of the oleic acid esterification with trimethylolpropane. *Journal of Chemical Technology and Metallurgy*, 57(6): 1104-1113.
- 32. Wahyudi, D., Fawzi, M., Cahyono, B., and Artanti, D. (2020). Influences of marine

- environment to the characteristics of palm oil biodiesel during storage. *Journal of Advanced Research in Fluid Mechanics and Thermal Sciences*, 79(1): 81-90.
- 33. Gordon, A. J., and Ford, R. A. (1973). The chemist's companion: A handbook of practical data, techniques, and references. John Wiley & Sons, Canada: pp. 448-452.
- 34. Ghodke, S., Dandekar, P., and Jain, R. (2021). Simplified evaluation aided by mathematical calculation for characterization of polyols by hydroxyl value determination. *International Journal of Polymer Analysis and Characterization*, 26(2): 169-178.
- 35. Bahadi, M., Salimon, J., and Derawi, D. (2021). Synthesis of di-trimethylolpropane tetraester-based biolubricant from *Elaeis guineensis* kernel oil via homogeneous acid-catalyzed transesterification. *Renewable Energy*, 171: 981-993.